NASA Technical Memorandum 81943

NASA-TM-81943 19810010368

EXPERIMENT REQUIREMENTS AND IMPLEMENTATION PLAN (ERIP) FOR SEMICONDUCTOR MATERIALS GROWTH IN LOW-G ENVIRONMENT EXPERIMENT NO. MPS 77F087

ROGER K. CROUCH, ARCHIBALD L. FRIPP, WILLIAM J. DEBNAM, AND IVAN O. CLARK

FEBRUARY 1981

NASA
National Aeronautics and Space Administration

Langley Research Center
Hampton, Virginia 23665

TABLE OF CONTENTS

LIST OF FIGURES

Figure

SUMMARY

The purpose of this program is to use the microgravity environment of orbital space flight systems to study the effects of gravity driven convection on the growth of $Pb_{1-x}Sn_xTe$ crystals. This document describes the need to eliminate convection, the furnace characteristics and operation that will be required for successful experimental implementation, and to the level that is presently known, the measured physical properties of the $Pb_{1-x}Sn_xTe$ system. In addition, a brief background of the present and potential utilization of $Pb_{1-x}Sn_xTe$ is given.

INTRODUCTION

Lead tin telluride is a narrow bandgap semiconductor material. The bandgap is adjustable from 0.21 ev to theoretically a zero bandgap by adjusting the ratio of the lead to tin on the metal side of the compound. This feature of PbSnTe makes it a desirable candidate for such applications as long wavelength infrared detectors and tunable diode lasers since these devices operate best when the wavelength of peak detectivity or emission is tailored to meet a specific need.

Both infrared detectors and tunable diode lasers have been built using PbSnTe but these devices have not yet been optimized for peak performance. The exact physics of device degradation due to crystalline defects is not complete; however, experience has helped to identify some of the interactions of defects and device characteristics.

Crystalline defects such as low angle gain boundaries and dislocations can produce diffusion paths which severely degrade diode junction characteristics and, hence, would be harmful to both detector and laser performance. Any compositional variations in the crystal will lower the peak detectivity of an infrared detector and can produce multimode emission from a laser. Strict control of the lattice dimension is necessary when the crystal is used as a substrate for epitaxial growth because a lattice mismatch produces strain in the crystal and this strain can be relieved by producing interfacial dislocations. Hence, the quality of the epitaxial device is limited by the quality of the starting material.

Since there is no commercial supplier of PbSnTe, device researchers and manufacturers must generally grow their own material. The three most common techniques of growth are:

1. Source ingot nucleation in which a polycrystalline aggragate is annealed for extended periods of time in an isothermal or nearly isothermal environment. Grain growth occurs during the anneal and small, highly faceted, low defect, crystals are produced.

2. Vapor transport in which PbSnTe vapor from a heated polycrystalline aggragate condenses on a slightly cooled, with respect to the source, substrate, Moderate sized crystals of moderate defect density are produced.

3. Liquid phase growth in which growth proceeds by controlled, directional solidification. This technique produces the largest crystals of the three techniques, but, to date, these crystals are the least homogeneous and exhibit the highest defect density.

Lead tin telluride single crystals can be grown on earth but as previously noted, the best quality crystlas are grown by the technique, ingot nucleation, which has the least interaction with the gravity field. The interaction of gravity on crystal growth is most evident in the liquid phase technique because the system, depending on growth orientation, will be either thermally or solutably unstable. The details of this instability will be discussed in the section on ground based research. The understanding of the interaction of gravity on crystal vapor growth is at a less mature state than the liquid growth but the present understanding centers around the establishment of a vapor diffusion boundary layer of included gases that must be supplanted in order for growth to occur.

The experiments discussed in this report will attempt to determine the effects of gravity on both the liquid phase and vapor phase growth techniques. With a better understanding of the growth mechanisms, the liquid and vapor techniques will be able to produce more nearly perfect crystals of PbSnTe.

LIST OF SYMBOLS

A_o	lattice constant, 10^{-10} meters
^oC	temperature, degrees Celsius
C_ℓ	solutal concentration of liquid phase, mole fraction
C_o	solutal concentration of starting material, mole fraction
C_s	solutal concentration of solid phase, mole fraction
D	solutal diffusion coefficient, $cm^2\ sec^{-1}$
g	acceleration due to gravity, $cm\ sec^{-2}$
G	temperature gradient, $^oC\ cm^{-1}$
G_s	solutal gradient, mole fraction cm^{-1}
H	dimension of furnace adiabatic zone, cm
k	segregation coefficient
L	characteristics length, cm
m	slope of liquidus line on phase diagram, ^oC mole fraction^{-1}
$N_{R_a}^S$	solutal Rayleigh number
$N_{R_a}^T$	thermal Rayleigh number
r	radial dimension, cm
R	growth velocity, $mm\ hr^{-1}$
t	time, minutes
T	temperature, ^oC
T_c	control set point of furnace cold zone, ^oC
T_H	control set point of furnace hot zone, ^oC
T_s	liquid-solid interface temperature, ^oC
V	volume, cm^3
X	concentration of SnTe in $Pb_{1-x}Sn_xTe$, mole fraction

z	axial coordinate, cm
β_T	coefficient of bulk thermal expansion, $^oC^{-1}$
β_x	coefficient of bulk solutal expansion, mole fraction^{-1}
λ	wavelength, 10^{-6} meters
ρ	density, gms cm^{-3}
ρ_ℓ	density of liquid phase, gms cm^{-3}
ρ_s	density of solid phase, gms cm^{-3}
ν	kinematic viscosity, cm^2 sec^{-1}

THE VALUE OF PROCESSING IN SPACE

The theory developed by Smith, Tiller, and Rutter (ref. 1) and Tiller et al (ref. 2) which defines the condition for steady state growth with no macroscopic segregation clearly requires that the liquid transport be diffusion controlled only. A horizontal growth configuration will have thresholdless convection; hence, vertical growth in the gravity field is required.

The composition of $Pn_{1-x}Sn_xTe$ which is of primary interest is (x) = 0.2. The liquid composition which will be in equilibrium with this solid is (x) = 0.29. Without considering, for the present, the effect of thermal dilatation, the density of liquid $Pb_{.71}Sn_{.29}Te$ at the growth interface will be approximately 0.98 times as massive as the undisturbed liquid five diffusion lengths into the melt. The maximum SnTe compositional gradient will be at the growth interface and is given by:

$$\frac{\partial C}{\partial Z} = -C_o \quad \frac{1 - k}{k} \quad \frac{R}{D} \tag{1}$$

Assume a nominal growth rate of 10 mm/hr and a liquid diffusion coefficient of $D = 7 \times 10^{-5}$ cm^2/sec, this gradient is

$$\frac{\partial C}{\partial Z} = -0.35 \frac{\text{mole fraction SnTe}}{\text{cm}} \tag{2}$$

The solutal Rayleigh number obtained with this concentration gradient and using a characteristic length of one centimeter is:

$$N_{R_a}^{S} = \frac{\beta'}{D\nu} g L^4 \frac{\partial C_\ell}{\partial Z} \tag{3}$$

$$N_{R_a}^{S} = 4.7 \times 10^8 \tag{4}$$

This extremely high Rayleigh number clearly exceeds any estimate of criticalness if the growth direction is antiparallel to the gravity vector.

A vertical growth parallel to the g-vector will have a thermally destabilizing configuration. Using the growth rate and diffusion coefficient used previously, a minimum thermal gradient of 25°C/cm at the growth interface, going into the liquid, is required to prevent constitutional supercooling. The earth-based thermal Rayleigh number for this gradient and a 1 cm characteristic length is:

$$N_{R_a}^{T} = \frac{\beta_\ell}{\alpha\nu} g L^4 \frac{\partial T}{\partial Z} \tag{5}$$

$$N_{R_a}^{T} = 3.2 \times 10^4 \tag{6}$$

This Rayleigh number must be decreased by a factor greater than 100 to fall below the generally accepted values of critical values. The characteristic length term, L, can only be decreased at the expense of crystal size and a

1 cm size is already at a minimum. The temperature growth rate can be decreased only by holding the ratio of temperature gradient and growth rate constant. That is:

$$\frac{1}{R}\ \frac{\partial T}{\partial Z} = \text{constant} \tag{7}$$

Hence, a large drop in $\partial T/\partial Z$ requires a large drop in R and a concomitant drop in the length of crystal growth needed to reach steady state which is given by

$$Z_{ss} = \frac{5D}{kR} \tag{8}$$

In a vertically upward growth an attempt can be made to metastabily balance the buoyancy of the excess SnTe at the interface with a thermally-expanded, due to steep temperature gradients, bulk melt. That is,

$$\frac{\partial \rho}{\partial Z} = \frac{\partial \rho}{\partial C}\ \frac{\partial C}{\partial Z} + \frac{\partial \rho}{\partial T}\ \frac{\partial T}{\partial Z} \leq 0 \tag{9}$$

let

$$\left| - \frac{\partial T}{\partial Z} \right| \geq \left| \frac{1}{\partial \rho / \partial T}\ \frac{\partial \rho}{\partial C}\ \frac{\partial C}{\partial Z} \right| \tag{10}$$

From available experiment values:

$$\frac{\partial \rho}{\partial T} = -8.43 \times 10^{-4} + 5.7 \times 10^{-5}\, C \quad \left[\frac{gm}{{}^{o}C\ cm^{3}}\right] \tag{11}$$

$$\frac{\partial \rho}{\partial C} = -1.667 + 5.7 \times 10^{-5}\, T \quad \left[\frac{gm}{cm^{3}\ \text{mole fraction}}\right] \tag{12}$$

and, from previous discussion in which $R = 10$ mm/hr and $D = 7 \times 10^{-5}$ cm^2/sec

$$\frac{\partial C}{\partial Z} = -0.35 \quad \frac{\text{mole fraction}}{cm} \tag{13}$$

Hence, for $C = 0.2$

$$\frac{\partial T}{\partial Z} \geq 680\ {}^{o}C/cm \tag{14}$$

or

$$\frac{G}{R} \geq 2.45 \times 10^{6} \quad \frac{{}^{o}C - sec}{cm^{2}} \tag{15}$$

These values of G and G/R are not obtainable in a crystal growth configuration and are certainly not obtainable in a configuration in which no radial gradients are allowed.

Hence, to obtain the theoretically prescribed conditions for stable crystal growth from the melt the crystal grower must reduce, preferable both, the solutal and the thermal Rayleigh numbers. The STS offers an ideal means to vary the Rayleigh numbers while maintaining centimeter dimensions on the crystal size.

FLIGHT EXPERIMENT DEFINITION

A. Liquid Phase Growth

The experiments are basically modifications of the subclass of directional solidification called Bridgman crystal growth. That is, all of the proposed liquid phase experiments will consist of PbSnTe contained in a fused quartz ampoule. A controlled amount of PbSnTe will be melted at the initiation of the experiment. Crystal growth will proceed by withdrawing the ampoule from the furnace hot zone.

One desired experiment will be packaged as shown schematically in figure 1. In this experiment, the contents of the entire ampoule are melted at experiment initiation. After a predetermined time to allow a completely thermal steady state condition to be reached the ampoule is slowly withdrawn from the hot zone, through the high temperature gradient, and into the cold zone. Solidification begins when a portion of the ampoule reaches the liquidous temperature and crystal growth is initiated. The initial growth may be polycrystalline, but the basic premise of Bridgman growth is that one polycrystalline grain will be in a more preferred growth orientation than the others, and hence, in the narrow constriction of the apex of the cone or in the recesses of the capillary the growth of the preferred grain will predominate and a single crystal will emerge.

Another desired liquid phase experiment will be packaged as shown in figure 2. This experiment is similar to the one described previously except that the single crystal seed is formed in the neck of the constricted region of the ampoule. The growth in the first to freeze region will be polycrystalline but grain growth will occur such that by the time the constricted

region is reached only one given grain will cover the orifice and hence a single crystal seed will be presented to the remainder of the ampoule.

The third type of liquid phase experiment will be a seeded Bridgman or a melt-regrowth experiment. This experiment will be packaged as shown in figure 3. In this experiment, at least a portion of the charge inside of the ampoule will be a single crystal. To initiate this experiment, the ampoule will be inserted into the hot zone only to the extent that a portion of the earth grown single crystal will be melted. The motion of the insertion mechanism is then reversed and the earth grown crystal serves as a seed for subsequent microgravity crystal growth.

All of the ampoules for the liquid phase experiments will have electrical connections for interfacial demarcation.

B. Vapor Phase Growth

The vapor phase experiments will be packaged in an ampoule as shown in figure 4. A high quality, single crystal, seed is fixed to the cold sink that extends out of the hot zone of the furnace. The polycrystalline ingot is at a higher temperature than the single crystal seed, hence, the difference in equilibrium vapor pressure over the polycrystalline ingot as compared to the seed will result in a net mass transfer to the seed and crystal growth will occur.

EXPERIMENT DEVELOPMENT

A. Theoretical Analysis of the Fluid System

For the best theoretical prediction of the thermal and fluid dynamic properties of crystal growth the coupled differential equations for conservation of momentum, energy, mass and species (the transport equations) must be applied to the system. This work, using finite element analysis, is being conducted by Fred Carlson and William R. Wilcox at Clarkson College. The energy equation converged quickly and the momentum equation coupled with the energy equation has been made to converge for simple geometries. This work will be continued to include the complete set of equations applied to the Bridgman configuration. Once the equations are made to converge for the Bridgman configuration, parameterization studies will be conducted to determine the accuracy with which thermophysical properties, such as heat conductivity, heat capacity and viscosity must be determined for accurate prediction of the fluid and heat transfer properties. An additional, and very important, parameter which will be studied will be the body force term in the momentum equation. In a stationary system on earth this body force term is the constant force due to gravity, whereas on the Space Shuttle the body force, even though greatly diminished from that on earth, may vary by orders of magnitude during the course of flight depending on activity aboard the spacecraft. The parameterization of the body force will allow the prediction of when reduced gravity can be considered "zero gravity."

Since the complete solutions, as outlined above, are not yet available, work has progressed at Langley on determination of system properties by using existing analytical solutions to one-dimensional models of directional solidification. The equations of interest are (refs. 2 and 3):

$$\frac{C_s}{C_o} = 1 - (1 - k)e^{-\frac{KR}{D}z} \tag{16}$$

and

$$\frac{G}{R} \geq \frac{C_s}{D} \frac{1 - k}{k} |m| \tag{17}$$

Equation (16) predicts the distance required to obtain uniform, homogeneous growth of a substitutional bindary alloy where no mixing other than diffusion occurs and equation (17) puts constraints on the growth parameters to avoid interfacial instability (constitutional supercooling). Note that equations (16) and (17) are coupled with respect to D, R and k. The phase diagram of PbSnTe exists (ref. 4); hence, the segregation coefficient and value of the liquidus slope exist and the liquid diffusion coefficient has been recently measured (ref. 5).

The relationships between R and G for two different values of D are given in table I. The value of G is not to be naively assumed to be equal to the slope of the empty furnace profile. This point will be discussed in the section on furnace design.

Dimensionless numbers are often used to characterize a fluid system. These dimensionless numbers are, in fact, parameters in the transport equations and their usefulness is much more obvious when used in that context. However,

TABLE I.- CALCULATIONS FOR LENGTH OF GROWTH TO ATTAIN STEADY-STATE COMPOSITION AND G/R RATIOS TO AVOID CONSTITUTIONAL SUPERCOOLING FOR VARIOUS GROWTH RATES AND DIFFUSION COEFFICIENTS

$D = 1 \times 10^{-5}$ cm^2 sec^{-1}			$D = 1 \times 10^{-4}$ cm^2 sec^{-1}		
Z_{ss}, cm	R, mm hr^{-1}	G, ^{o}C cm^{-1}	Z_{ss}, cm	R, mm hr^{-1}	G, ^{o}C cm^{-1}
0.25	10.4	286	0.25	104.4	286
0.5	5.0	143	0.5	50	143
0.75	3.4	95	0.75	34	95
1.0	2.6	21.6	1.0	26	71.6
1.5	1.7	47.7	1.5	17	47.7
2.0	1.3	35.8	2.0	13	35.8
2.5	1.0	28.6	2.5	10	28.6
3.0	0.86	23.6	3.0	8.6	23.6
5.0	0.5	14.3	5.0	5	14.3
10.0	0.26	7.2	10.0	2.6	7.2

lacking, for the present, the complete solutions for the transport equations the thermal and solutal Rayleigh numbers have been studied.

These numbers are defined by the equations below:

$$N_{R_a}^{T} = \frac{\beta\, G L^4}{\alpha \nu}\, g \tag{18}$$

and

$$N_{R_a}^{S} = \frac{\beta'\, G_s L^4}{D\nu}\, g. \tag{19}$$

The Rayleigh number can be considered to be the driving force for convection where the mass imbalance vector is antiparallel to the body force vector. That is, the $\beta_T G g$ or $\beta_x G_s g$ term induces convection and the viscous interaction with the walls retards convection. The effects of surface tension are ignored; hence, these numbers do not predict the observation that a liquid can be retained in a pinched soda straw.

B. Determination of Growth Parameters

The one-dimensional theory (eqs. (18) and (19)) mentioned in part A requires that the liquid diffusion coefficient and the phase diagram be known before growth parameters such as growth rate and temperature gradient can be chosen. However, the temperature gradient can only be estimated until the complete set of transport equations are solved.

Effort will continue on solving the complete set of transport equations and parameterizing the thermophysical coefficients to determine the accuracy

to which they need to be measured. The more accurate data can then be fed back into the equation to determine the furnace wall temperature profile required to maintain a planar liquid solid interface during the growth process. It is anticipated that the furnace profile as well as the desired interface temperature will decrease as a function of time during the transient growth period.

B. Furnace Design

It was recognized early in this program that a furnace with a high temperature gradient would be required for Bridgman crystal growth. Multi-zone furnaces have been built, both with and without isothermal liners. A technical journal article describing the furnaces and their thermal characteristics is in preparation; hence, the work will only be summarized at this time.

The temperature profiles as recorded by both bare thermocouples and thermocouples imbedded in a boron nitride rod were measured. The furnace was constructed as shown schematically in figure 5. Runs were made with variables being end point temperatures, type and thickness of intervening insulation, presence or absence of quartz liner, orientation of furnace, atmosphere within liner and, most importantly, the effect of isothermal liners. Typical data are shown in figures 6 and 7.

The work performed on the furnace has made it very obvious that the slope of a bare thermocouple reading versus distance in the furnace is not the temperature gradient within the liquid of a crystal growth system. The desire to obtain the needed temperature gradient within the liquid phase plus the need to maintain a planar isotherm at the solidification temperature will

require a interaction between furnace designers and crystal growers. That is, the maximum obtainable temperature gradient in a given furnace is a function of the difference in temperature between the "hot" and "cold" zones and whereas the shapes and positions of the isotherms are a function of the furnace design and the ampoule properties.

Another area that has been theoretically investigated is the effect of furnace stability, both thermal control and pull rate control, on the homogeneity of the directionally solidified crystals. Since the thickness of the diffusion boundary layer is a function of growth rate, any change in growth rate will produce a change in solute distribution between the solid and liquid phases if the initial melt composition is uniform and steady state growth was proceeding without mixing in the liquid other than diffusion away from the advancing interace.

The equation for perturbed distribution due to growth rate changes as derived by Smith et al (ref. 1) is:

$$\frac{C_S(z_1)}{C_o} = 1 - \frac{1}{2}\,\mathrm{erfc}\left(\frac{(R_1/D)z_1}{4}\right)^{\frac{1}{2}} + q\left(\frac{1/2 - R/R_1}{k - R/R_1}\right)$$

$$\times \exp\left[-\frac{R}{R_1}\left(1 - \frac{R}{R_1}\right)\frac{R_1}{D}z_1\right]\mathrm{erfc}\left[\left(\frac{R}{R_1} - \frac{1}{2}\right)\left(\frac{R_1}{D}z_1\right)^{\frac{1}{2}}\right]$$

$$+ \left(\frac{2k - 1}{2}\right)\left(\frac{1 - R/R_1}{k - R/R_1}\right)\exp\left(-k\,q\,\frac{R_1}{D}z_1\right)$$

$$\mathrm{erfc}\left[\left(k - \frac{1}{2}\right)\left(\frac{R_1}{D}z_1\right)^{\frac{1}{2}}\right]. \qquad (20)$$

where

$q = 1 - k$

z_1 = the distance from the point at which the speed change occurred

R_1 = new growth rate.

The result is an initial rapid change in solid composition as the diffusion barrier redistributes itself, the compositional change peaks and then slowly settles back to the steady state distribution of $C_s = C_o$.

The growth rate can be change by either of two mechanisms. The actual pull rate of the crystal can vary due to the drive mechanism or the temperature of the furnace can vary which will change the position of the freezing isotherm causing a transient change in growth rate.

The analysis of tolerable furnace stability will proceed as follows:

The required compositional control is determined by device performance requirements and by the ability to measure changes in composition.

After C_s/C_o maximum has been determined the growth rate (R/R_1) changes that can produce the compositional change are determined by plotting equation (20) as a function of $R_1 z_1/D$ where, of course, R/R_1 is a parameter. The mechanisms, pull rate stability and temperature control stability, are then examined to determine the requirements for uniform composition in crystal growth.

The desired ratios of lead to tin in the compound is determined by the wavelength of desired peak detectivity in infrared detector applications. Potential applications are generally for detection of wavelengths of between 6 and 18 μm which require a tin to lead percentage of between 3 and 30 percent. For purposes of comparison a 20 percent tin/80 percent lead composition

(λ_{co} = 10 μm) with an allowed 0.25 μm variation in λ_{co} will be used. Equation (21) gives the allowed compositional variation for such a detector.

$$\Delta X = \frac{-1.24\ \Delta\lambda}{\lambda_{co}^2[Eg(PbTe) - Eg(SnTe)]} \quad \text{(ref. 6)} \tag{21}$$

Hence

$$\Delta X = 0.0065$$

or

$$C_s/C_o = 1.032$$

The compositional variation, C_s/C_o is plotted as a function of the non-dimensional parameter, $Z = R_1\ z_1/D$ in figure 8. The maximum compositional variation versus R/R_1 is plotted in figure 9. For the aforementioned compositional uniformity requirement only values of R/R_1 less than 0.75 need be considered.

As can be seen in figure 8, the maximum compositional change does not occur immediately. This will be an important observation for the discussion of thermal stability.

Thermal stability affects the growth rate by changing the physical position of the solidus isotherm. Consider the one-dimensional model in which the hot side of the furnace goes from T_H to $T_H - \Delta T$. The position of the solidus, as an first order effect, will move by an amount:

$$\Delta z = H \frac{T_s - T_c}{T_H - \Delta T - T_c} \frac{\Delta T}{T_H - T_c} . \tag{22}$$

If ΔT is small compared to $T_H - T_c$ then:

$$\Delta z \approx \frac{T_s - T_c}{(T_H - T_c)^2} H \Delta T \tag{23}$$

Instantaneous temperature changes are not expected, however ramp changes may occur. That is, the temperature may change as a function of time such that the new growth rate, R_1, may be expressed as:

$$R_1 = R + \frac{\Delta z}{\Delta t} \tag{24}$$

or

$$R_1 = R + \frac{T_s - T_L}{(T_H - T_L)^2} H \frac{\Delta T}{\Delta t} \tag{25}$$

where $\Delta T/\Delta t$ is the time rate of change of the furnace temperature.

The exact values for the parameters, other than T_s, in equation (25) are, as yet, not determined but approximate values can be estimated as:

$T_H = 1100^\circ$ C

$T_C = 500^\circ$ C

$H = 4$ cm

The values of T_s for the composition of interest is 890° C. The desired growth rate is expected to be between 2 and 20 mm/hour. Using these parameters and noting that the ratio of R to R_1 must not be less than 0.75, the temperature stability can be calculated by solving equation (25) for $\Delta T/\Delta t$. That is:

$$\frac{\Delta T}{\Delta t} = \frac{R_1 - R}{H} \frac{(T_N - T_C)^2}{(T_s - T_C)} \tag{26}$$

$$\frac{\Delta T}{\Delta t} = \frac{1 - R/R_1}{R/R_1} \frac{R}{H} \frac{(T_H - T_C)^2}{(T_s - T_C)} \tag{27}$$

if $R/R_1 = 0.75$, then

$$\frac{\Delta T}{\Delta t} = \frac{R}{3H} \frac{(T_N - T_C)^2}{T_s - T_C} \tag{28}$$

or

$$\frac{\Delta T}{\Delta t} = \frac{.25R_1}{H} \frac{(T_H - T_C)^2}{T_s - T_C} \tag{29}$$

then

$$\frac{\Delta T}{\Delta t} \leq \begin{cases} 15.2^{\circ}\ C/hr,\ R = 2.0\ mm/hr \\ \\ 152^{\circ}\ C/hr,\ R = 20\ mm/hr \end{cases}$$

As mentioned earlier, the maximum compositional change does not occur immediately. As can be seen in figure 8, the same compositional change occurs when the dimensionless parameter, z equals 0.25 if $R/R_1 = 0.7$ as when z equals 0.7 is $R/R_1 = 0.75$. Hence, for a given furnace instability, the time needed for the maximum effect to take place is dependent on the initial growth rate and on the liquid diffusion coefficient.

Referring to the more tolerant level of $R/R_1 = 0.75$ the temperature perturbation would have to exist for a time such that

$$t_1 = 0.7 \frac{D}{R_1^2} \tag{30}$$

which is obtained by considering that:

$$Z_{crit} = 0.7$$

hence,

$$Z_1 = 0.7 \frac{D}{R_1} \tag{31}$$

since

$$z_1 = R_1 t_1$$

then

$$t_1 = Z_{crit} \frac{D}{R_1^2} \tag{32}$$

or

$$t_1 = 0.7 \frac{D}{R_1^2} .$$

The time of the perturbation necessary to peak C_s/C_o-versus-z_1 can be expressed in terms of R instead of R_1. That is:

$$t_1 = Z_{crit} D \left(\frac{R}{R_1}\right)^2 \frac{1}{R^2} \tag{33}$$

where (R/R_1) = constant. If $R/R_1 = 0.75$ and $Z_{crit} = 0.7$ then

$$t_1 = 1.24 \frac{D}{R^2} \tag{34}$$

if $D = 7 \times 10^{-5}$ cm^2/sec (0.25 cm^2/hr) then

$$t_1 = \begin{cases} 2.46 \text{ hr, } R = 20 \text{ mm/hr, } \Delta T/\Delta t = 15.2^{\circ} \text{ C/hr} \\ .0246 \text{ hr, } R = 20 \text{ mm/hr, } \Delta T/\Delta t = 152^{\circ} \text{ C/hr} \end{cases}$$

where

t_1 = the time after temperature perturbation started.

The value of the dimensionless parameter, $Z = R_1/D\ z_1$, required to produce a compositional change equal to $C_s(z)/C_o = 1.032$ decreases rapidly as R/R_1 decreases. This relationship is shown in figure 10. The time duration of the perturbation as a function of the amplitude of the perturbation (R/R_1) to produce the compositional change of $C_s/C_o = 1.032$ can be calculated as follows:

$$t_{crit} = \frac{D}{R_1^2} Z_{crit} \tag{35}$$

where Z_{crit} is taken from figure 10.

The cause of the growth rate change is the temperature rate of change, which for a given R and R/R_1 can be calculated from equation (27). The relationship between $\Delta T/\Delta t$ and t_{crit} is plotted in figure 11.

C. Interfacial Demarcation

The implementation of interfacial demarcation requires electrical connections through each end of the quartz ampoule, short but sufficiently intense current pulses through the growing medium, and an etchant technique capable of displaying the effects of the electrical pulsing. Effort is currently underway toward fulfillment of all of these areas and limited success has been obtained.

FURNACE REQUIREMENTS FOR MPS EXPERIMENTS

The furnace requirements are given in table II.

TABLE II.- FURNACE REQUIREMENTS

Requirement	Experiment	
	Liquid	Vapor
Operating Range	300 to 1200° C	500 - 900° C
Ampoule Size	0.8 cm ID	
	1.2 cm OD	1 - 2.5 cm OD
	2.5 cm long	6 - 25 cm long
Heated Cavity Control		
Control setpoint stab.	±0.05%(1)	0.1° C differential
Control setpoint stab. rate	<1° C/hr in sample(1)	
Control setpoint accuracy	±0.5%(1)	±5° C
Time to temp.	≤1 hr	≤30 min w/o gradient reverse, 1 hr with reverse
Temp. overshoot - hot end	20° C	≤5° C
Temp. overshoot - cold end	20°C	≤5°C
Stabilization time	<10 min	N/R
Axial gradient at interface	100° C/cm - min 400° C/cm - desired	N/A
Linear gradient range	N/A	3 - 25° C rev.
		6 - 50° C forward(2)
Axial gradient stab.	(1)	N/A
Linear gradient zone length	N/A	25 cm
Axial grad. measuring distance	≤5 mm	N/A

TABLE II.- Continued

Requirement	Experiment	
	Liquid	Vapor
Radial gradient	(1)	$\pm 0.25^{\circ}$ C/cm
Circumferential gradient at solidification interface	±0.05% of axial gradient at interface	0.25° C/cm
Translation of Ampoule		
Rate - range	0.3 - 50 mm/hr	NR
Rate change within area	5 - 10	NR
Rate change disturb time	5 sec max	NR
Rate change overshoot	$<10^{-4}$ g	NR
Rate stability	<1%	NR
Rate stability rate	<1.0 mm/sec^2	
Cooling Requirements		
Temp. reduction rate	Passive cooling is OK	$0 - 60^{\circ}$C/min until $T < 500^{\circ}$ C then quench is OK
Operating Environment	He	He
Peltier Pulsing		
Current, range	.5 to 16 amps	NA
Absolute accuracy	±10%	NA
Repeatability	±1%	NA
Stability	±5%	NA
Selectivity	5	NA
Voltage	<20 volts	NA
Pulse width, range	0.1 to 5 sec	NA

TABLE II.- Continued

Requirement	Experiment	
	Liquid	Vapor
Absolute accuracy	±5%	NA
Repeatability	±1%	NA
Rise time	1 to 5% of pulse width	NA
Selectivity	Factor of 2 of selected pulse width	NA
Pulse interval, range	1 to 300 sec	NA
Absolute accuracy	±5%	NA
Repeatability	±1%	NA
Selectivity	2X, 5X, and 10X of pulse interval	NA
Temperature Measurements		
Absolute accuracy	$\pm 1^{\circ}$ C	$\pm 1^{\circ}$ C
Resolution	0.1° C	0.15° C differential
Data rate	1 sps	1 sps
No. of sensors	6	6
Ampoule Material	quartz, graphite, moly	quartz
Special Data		
Residual Accel.		
Linear	$\leq 1 \times 10^{-5}$ g_e	$\leq 1 \times 10^{-5}$ g_e
Radial	$\leq 1 \times 10^{-4}$ radian/sec^2	$\leq 1 \times 10^{-4}$ radian/sec^2

TABLE II.- Concluded

NOTE 1

Furnace parameters such as control setpoint accuracy, control setpoint stability and axial gradient stability are interrelated and are primarily important as to how they affect the position of the solid-liquid interface. The temperatures of the hot and cold zones are set to produce a planar interface. The interaction of the furnace design and the physical properties of the experiment will determine what magnitude of control is necessary to maintain the planar interface.

NOTE 2

An example of minimum gradient ΔT's are 850°C at the source, 853° C at the ampoule midpoint and 847° C at the seed.

DESCRIPTION OF EXPERIMENT SPECIMENS

A. Composition

1. Liquid growth - nominal values

52.3 wgt % lead

7.5 wgt % tin

40.2 wgt % tellurium

2. Vapor growth - nominal values

52.3 wgt % lead

7.5 wgt % tin

40.2 wgt % tellurium

The above values are nominal as the maximum melting point, and possibly, the most congruent vaporization point of the binary end point compounds are tellurium rich.

B. Size

1. Liquid growth

1.2 cm OD, 25 cm long

2. Vapor growth

1 - 2.5 cm OD, 6 - 25 cm long

C. Weight

1. Liquid growth

120 grams

2. Vapor growth

70 grams

D. Materials

1. Sample $Pb_xSn_{1-x}Te$

2. Ampoule

   Quartz with moly feedthroughs and graphite inserts

3. Thermocouple probes

   Type K in inconel sheaths

E. Materials Characteristics of PbTe, SnTe and $Pb_xSn_{1-x}Te$

1. Thermal conductivity (ref. 7)

$Pb_{.8}Sn_{.2}Te$

T(°C)	K (W cm^{-1} K^{-1})
22	1.47×10^{-2}
100	1.24×10^{-2}
150	1.17×10^{-2}
200	1.12×10^{-2}
220	1.11×10^{-2}
300	1.32×10^{-2}
400	1.65×10^{-2}
500	1.91×10^{-2}
600	2.08×10^{-2}
700	2.22×10^{-2}
750	2.28×10^{-2}

PbTe and SnTe - The tabulated data were taken from curves in reference 8.

	PbTe	SnTe
T(^{o}C)	K(W cm^{-1} K^{-1})	K(W cm^{-1} K^{-1})
325	x 10^{-2}	
425	x 10^{-2}	2.0 x 10^{-2}
525	1.0 x 10^{-2}	1.7 x 10^{-2}
625	1.2 x 10^{-2}	1.7 x 10^{-2}
725	1.3 x 10^{-2}	2.7 x 10^{-2}
775	1.7 x 10^{-2}	3.4 x 10^{-2}
Tm SnTe		4.0 x 10^{-2} solid
"		5.3 x 10^{-2} liquid
825	2.0 x 10^{-2}	5.3 x 10^{-2}
875	2.7 x 10^{-2}	6.0 x 10^{-2}
Tm PbTe	4.5 x 10^{-2} solid	
	5.3 x 10^{-2} liquid	
975	6.0 x 10^{-2}	7.3 x 10^{-2}
1075	7.2 x 10^{-2}	8.3 x 10^{-2}
1175	8.4 x 10^{-2}	9.3 x 10^{-2}

Specific Heat

$Pb_{.8}Sn_{.2}Te$ (ref. 7)

T(^{o}C)	Cp (W sec gm^{-1} K^{-1})
22	0.1605
500	0.1720
700	0.1816
750	0.1836

Heat of Fusion

SnTe 5.4 K cal/mole (ref. 9)

PbTe 3.75 K cal/mole (ref. 10)

The heat of fusion for PbTe was only quoted in reference 10, and it was impossible to verify it by looking at the English version of their original source.

Density

The measured densities of solid and liquid PbTe and SnTe are easily fitted to a slope-intercept equation. That is:

$$\rho_i = A_i + B_i T, \qquad T \text{ is in } {}^{o}C$$

The values of A and B are: (ref. 11)

Material	A_i	B_i
PbTe solid	8.192	-5.38×10^{-4}
PbTe liquid	8.181	-8.43×10^{-4}
SnTe solid	6.467	-4.29×10^{-4}
SnTe liquid	6.514	-7.86×10^{-4}

The density of pseudobinary alloy of (1 - X) mole fraction PbTe and X mole fraction SnTe is:

$$\rho(X,T) = (1-X)\left[\frac{A_o(PbTe)}{A_o(Pb_{1-x}Sn_xTe)}\right]^3 \rho_{PbTe}^{(T)}$$

$$+ X\left[\frac{A_o(SnTe)}{A_o(Pb_{1-x}Sn_xTe)}\right]^3 \rho_{SnTe}^{(T)}$$

At the composition and temperature ranges of interest an error of less than 1 percent is incurred by using

$$\rho(X,T) = (1 - X)\rho_{PbTe}^{(T)} + X\,\rho_{SnTe}^{(T)}$$

Coefficient of Bulk Thermal Expansion

This parameter is defined as:

$$\beta_T = \frac{1}{v}\frac{\partial v}{\partial T}$$

or

$$\beta_T = -\frac{1}{\rho}\frac{\partial \rho}{\partial T}$$

which reduces to

$$\beta_T = - \frac{1}{\rho_{(X,T)}} \left[(1 - X) \; B_{PbTe} + X \; B_{SnTe} \right]$$

for the alloy.

Values of the bulk thermal coefficient of expansion of $Pb_{.8}Sn_{.2}Te$ are:

Solid (890° C)

$$\beta_T = 68 \times 10^{-6}/^{\circ}C$$

Liquid (905° C)

$$\beta_T = 113 \times 10^{-6}/^{\circ}C$$

This term is analogous to the thermal coefficient of expansion and is defined as:

$$\beta_X = \frac{1}{v} \frac{\partial v}{\partial X}$$

or

$$\beta_X = - \frac{1}{\rho} \frac{\partial \rho}{\partial X}$$

which reduces to

$$\beta_X = \frac{\rho_{SnTe}^{(T)} - \rho_{PbTe}^{(T)}}{(1 - X)\rho_{PbTe}^{(T)} + X\,\rho_{SnTe}^{(X)}}$$

for the alloy.

Selected values for $Pb_{.8}Sn_{.2}Te$ are:

Solid (890 °C)

β_X = -0.22/mole fraction of SnTe

Liquid (905 °C)

β_X = -0.23/mole fraction of SnTe.

Viscosity (ref. 10)

Temperature (°C)	Kinematic Viscosity (cm^2/sec) PbTe	SnTe
830		3.48×10^{-3}
865		3.26×10^{-3}
915		2.68×10^{-3}
940	2.43×10^{-3}	
965		2.16×10^{-3}
970	2.16×10^{-3}	
980	2.17×10^{-3}	
1000	2.03×10^{-3}	
1010		2.02×10^{-3}
1020	1.90×10^{-3}	
1050		1.98×10^{-3}
1060	1.73×10^{-3}	
1090	1.68×10^{-3}	1.89×10^{-3}
1100	1.57×10^{-3}	
1130		1.84×10^{-3}
1140	1.42×10^{-3}	
1170		1.82×10^{-3}
1180	1.34×10^{-3}	
1190	1.46×10^{-3}	
1210		1.75×10^{-3}
1230	1.34×10^{-3}	

SAFETY CONSIDERATIONS

The experiments described in this document present no risks of fire, explosion, high pressure glass breakage or, at room temperature, toxicity. However, both lead and tellurium emit toxic fumes at elevated temperatures. The accepted, long term exposure per cubic meter of air is 0.2 milligram for lead and 0.1 milligram for tellurium (ref. 12). These levels exist at 500 ^{o}C and 300^{o} C, respectively, over the elements. However, PbTe does not dissociate in the vapor state and its vapor pressure is approximately equal to that of lead. Consequently, dangerous levels of PbTe will condense on surfaces which are cooler than 500^{o} C.

MILESTONES

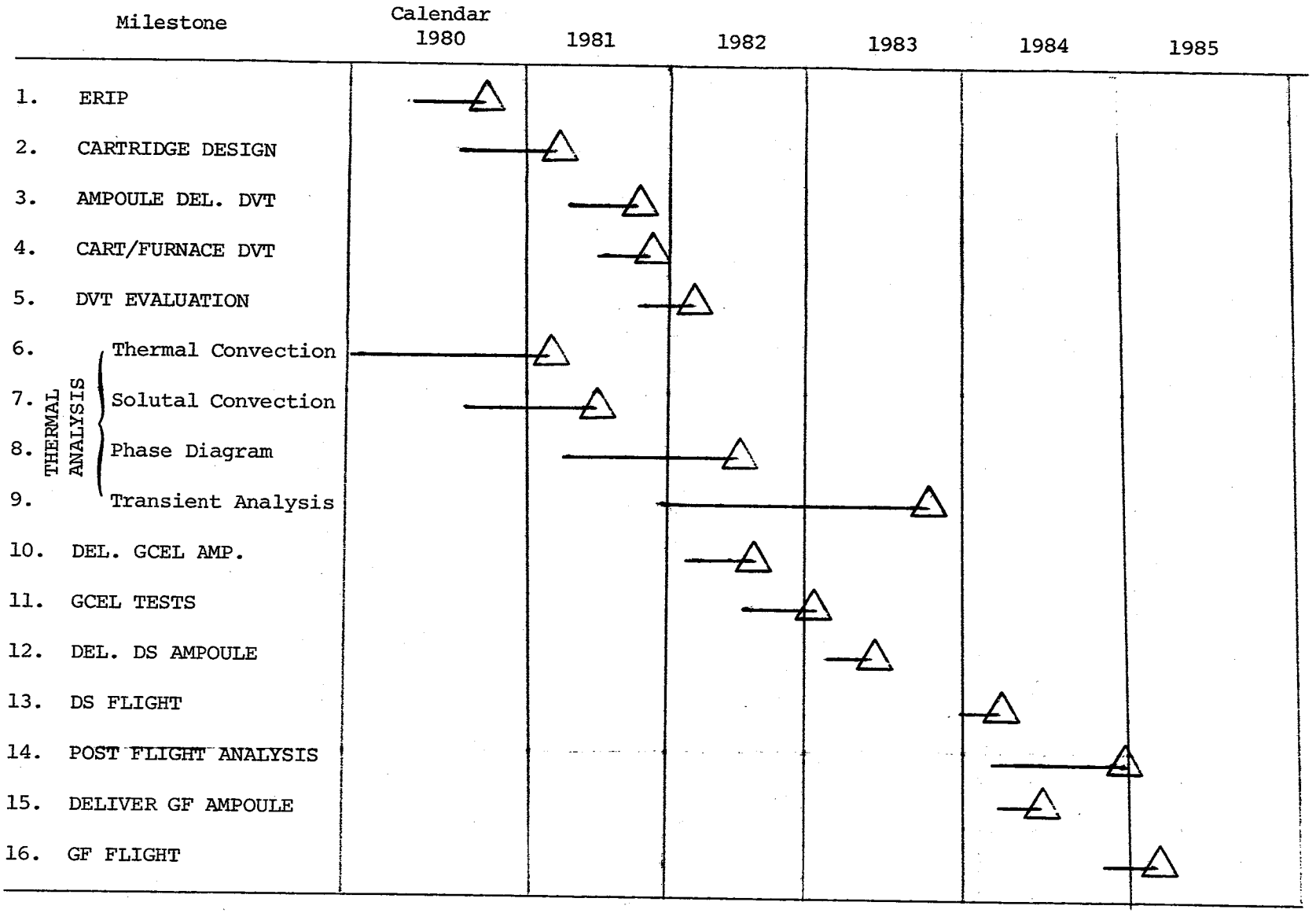
Milestone
Calendar
1980
1981
1982
1983
1984
1985
1. ERIP
2. CARTRIDGE DESIGN
3. AMPOULE DEL. DVT
4. CART/FURNACE DVT
5. DVT EVALUATION
6. Thermal Convection
7. Solutal Convection
8. Phase Diagram
9. Transient Analysis
THERMAL ANALYSIS
10. DEL. GCEL AMP.
11. GCEL TESTS
12. DEL. DS AMPOULE
13. DS FLIGHT
14. POST FLIGHT ANALYSIS
15. DELIVER GF AMPOULE
16. GF FLIGHT

REFERENCES

1. V. G. Smith, W. A. Tiller, J. W. Rutter: Candian J. Phys., 33, 723 (1955).

2. W. A. Tiller, K. A. Jackson, J. W. Rutter, and B. Chalmers: Acta. Met. 1, 428 (1953).

3. W. A. Tiller and J. W. Rutter: Canadian J. Phys., 34, 96 (1956).

4. A. R. Calawa, T. C. Harman, M. Finn, and P. Youta: Trans. Met. Soc. AIME, 242, 374 (1968).

5. I. O. Clark, A. L. Fripp, W. J. Debnam, and R. K. Crouch: J. Electrochem. Soc., 127, 137C (1980).

6. A. L. Fripp and R. K. Crouch: I. R. Phys., 19, 701 (1979).

7. R. E. Taylor and H. Groot: Report No. TPRL 203, Thermophysical Properties Research Laboratory, Purdue University, West Lafayette, Indiana.

8. V. I. Fedorov and V. I. Machuev, Soviet Physics - Solid States, 11, 1116 (1969).

9. R. F. Brebrick and A. J. Strauss, J. Chem. Phys., 41, 197 (1964).

10. N. N. Glagoleva, A. N. Krestovnikou, and V. M. Glazov, Inorganic Materials, 4, 1647 (1968).

11. V. M. Glazov, S. N. Chizhevskaya, and N. N. Glagoleva: Liquid Semiconductors, Plenum Press, NY, 1969.

12. N. I. Sax: Dangerous Properties of Industrial Materials, Reinhold Publishing Corp., NY (1963).

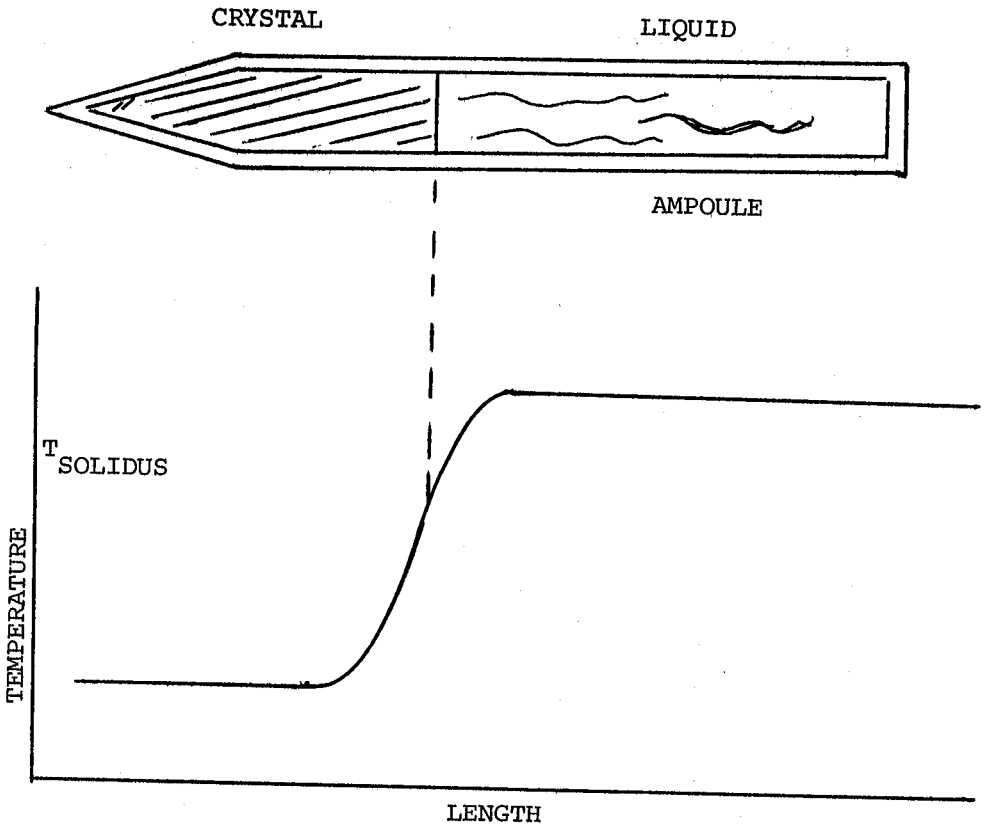

Figure 1.- Bridgman growth configuration - conical end.

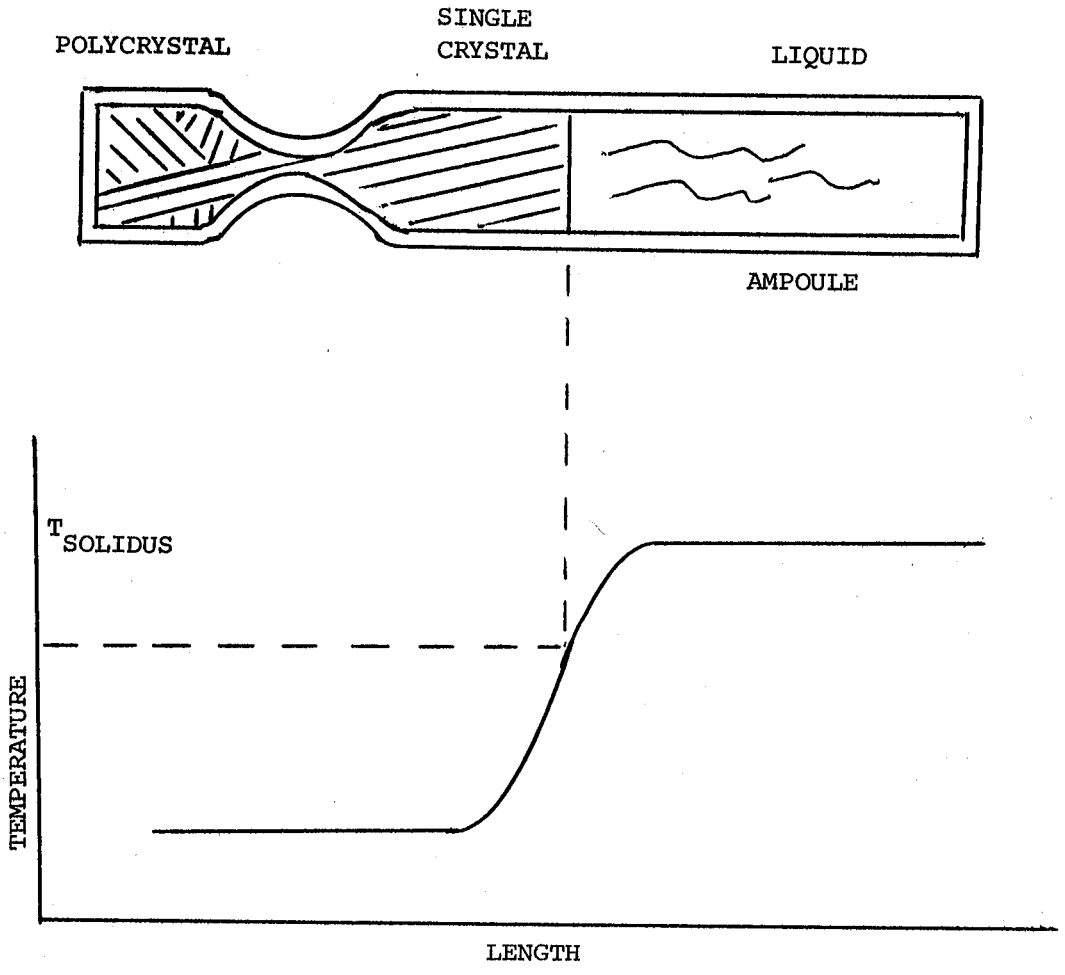

Figure 2.- Bridgman growth configuration - necked end.

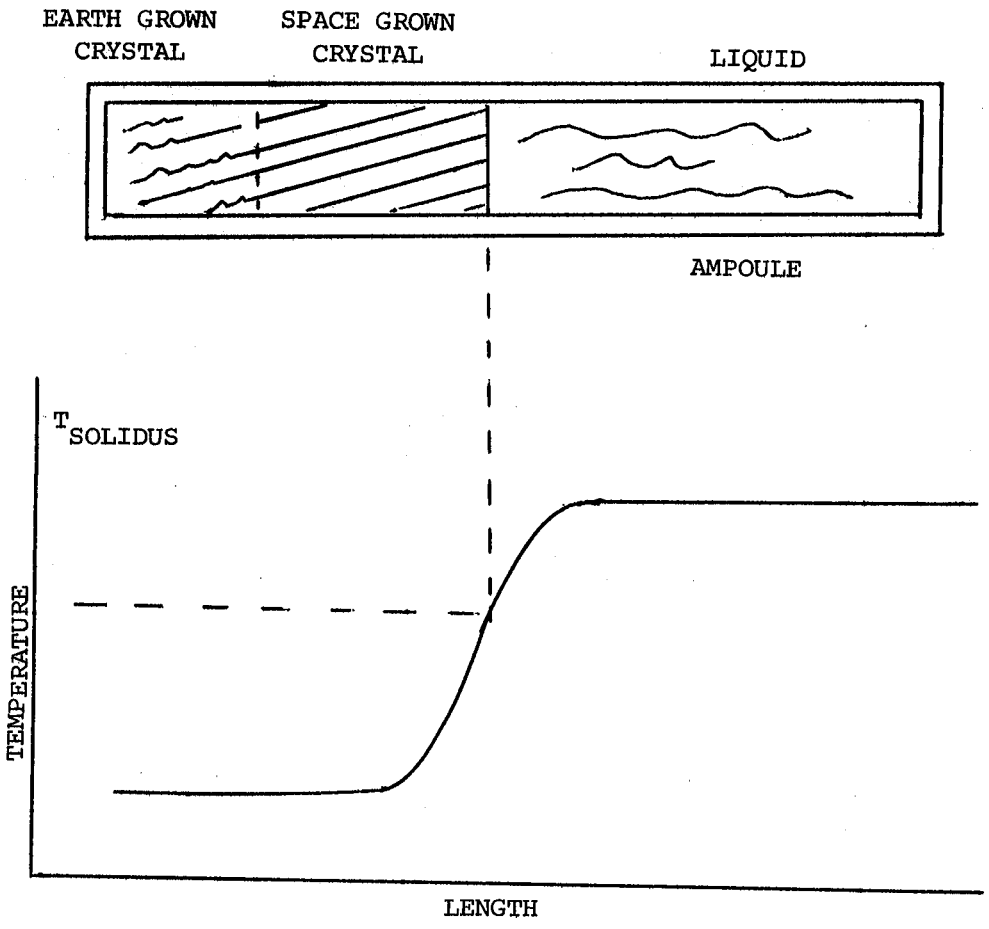

Figure 3.- Seeded Bridgman growth configuration.

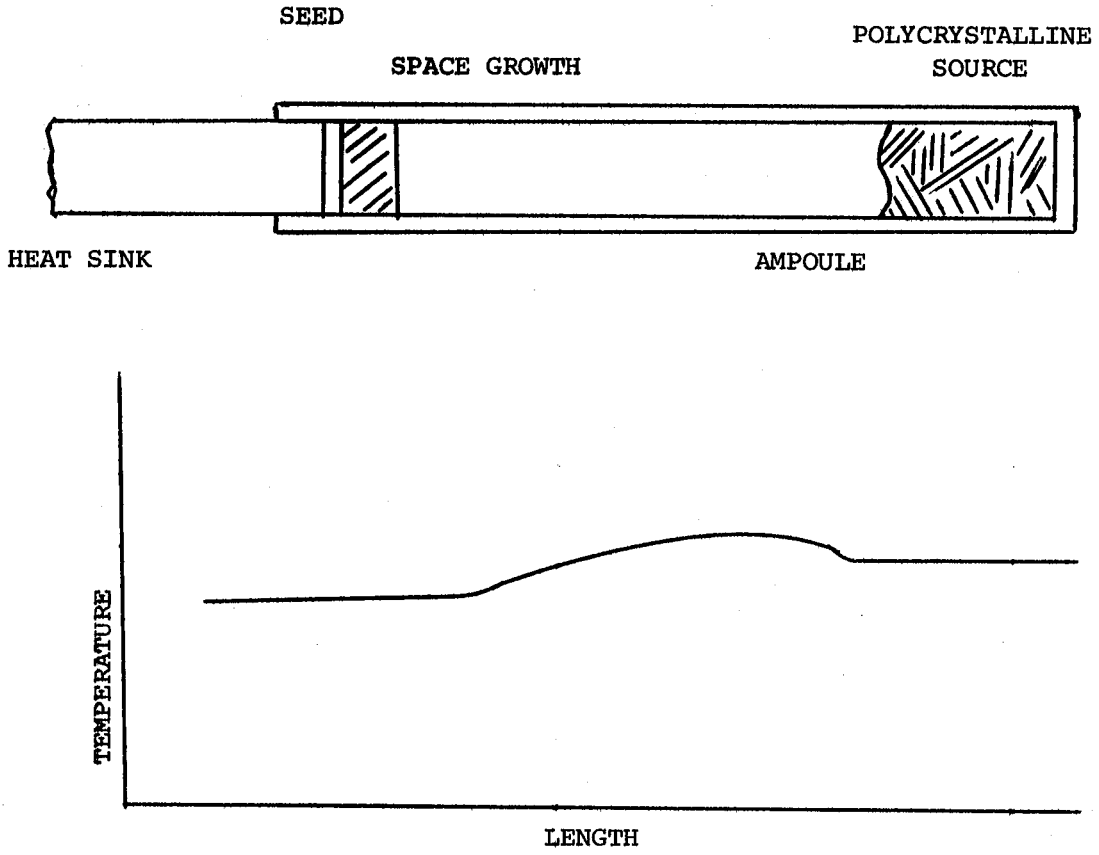

Figure 4.- Vapor growth configuration.

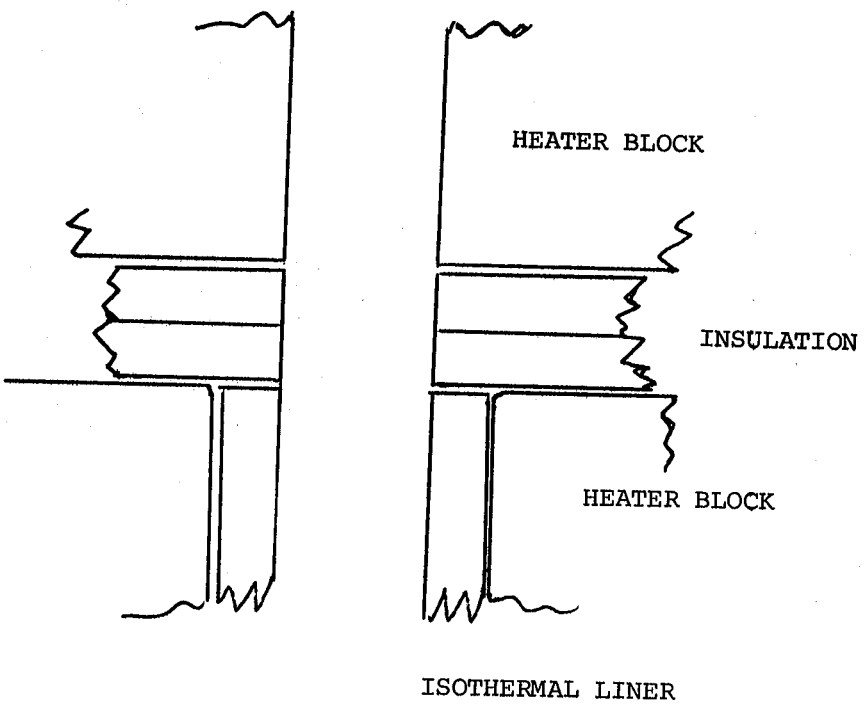

Figure 5.- Schematic of directional solidification furnace.

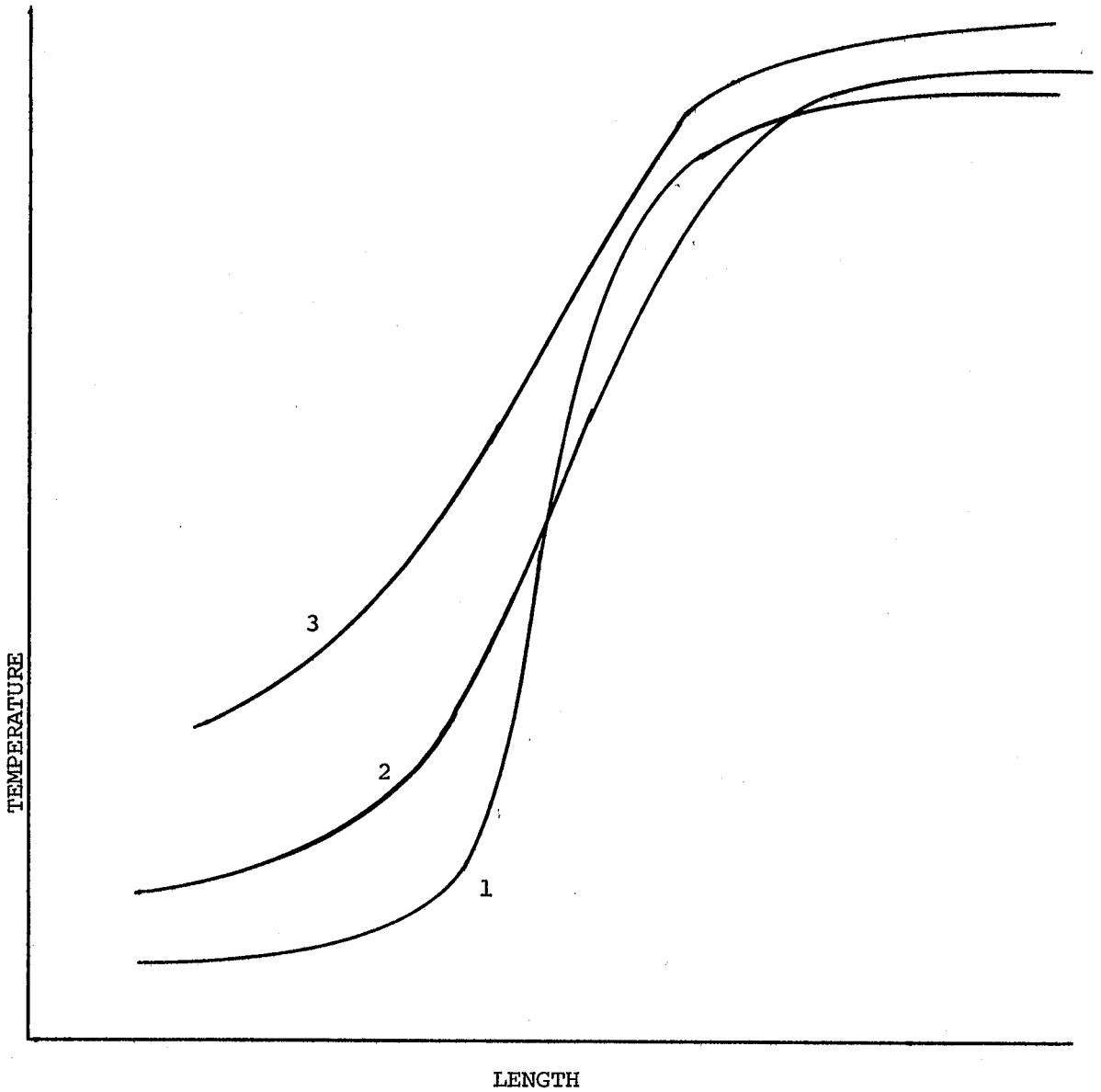

Figure 6.- Examples of empty furnace profiles obtained in ground-base research. All data were taken under similar circumstances except as noted. Curve 1, 1.25 cm orifice between zones. Curve 2, 218 cm OD quartz tube in place. Curve 3, 3.18 OD quartz tube in place and no isothermal liner.

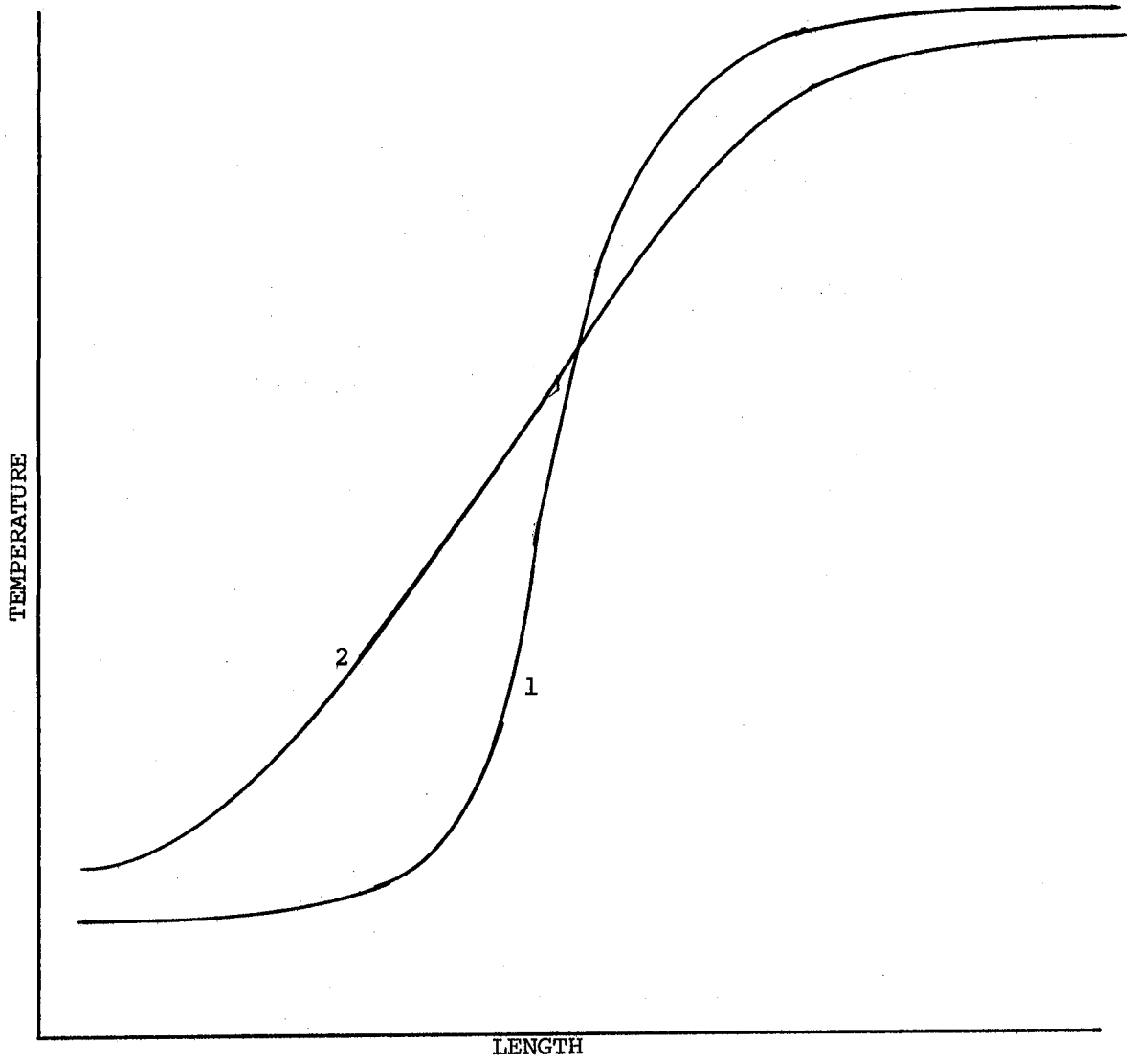

Figure 7.- Examples of furnace profiles obtained in ground-based research. Data for both curves were taken under similar circumstances except that curve 1 is a thermocouple in an empty furnace and curve 2 is a thermalcouple embedded in a boron nitride rod.

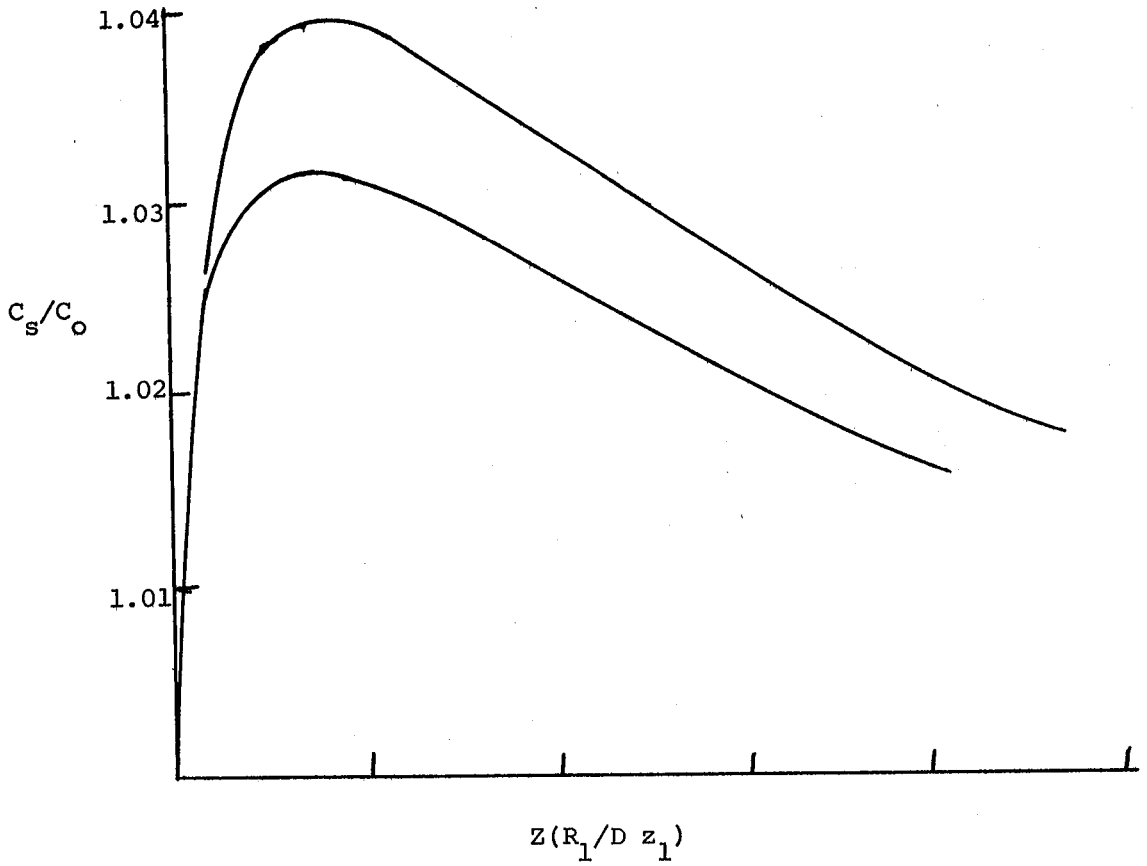

Figure 8.- Calculated composition (of solid) change a growth rate change for $Pb_{.8}Sn_{.2}Te$.

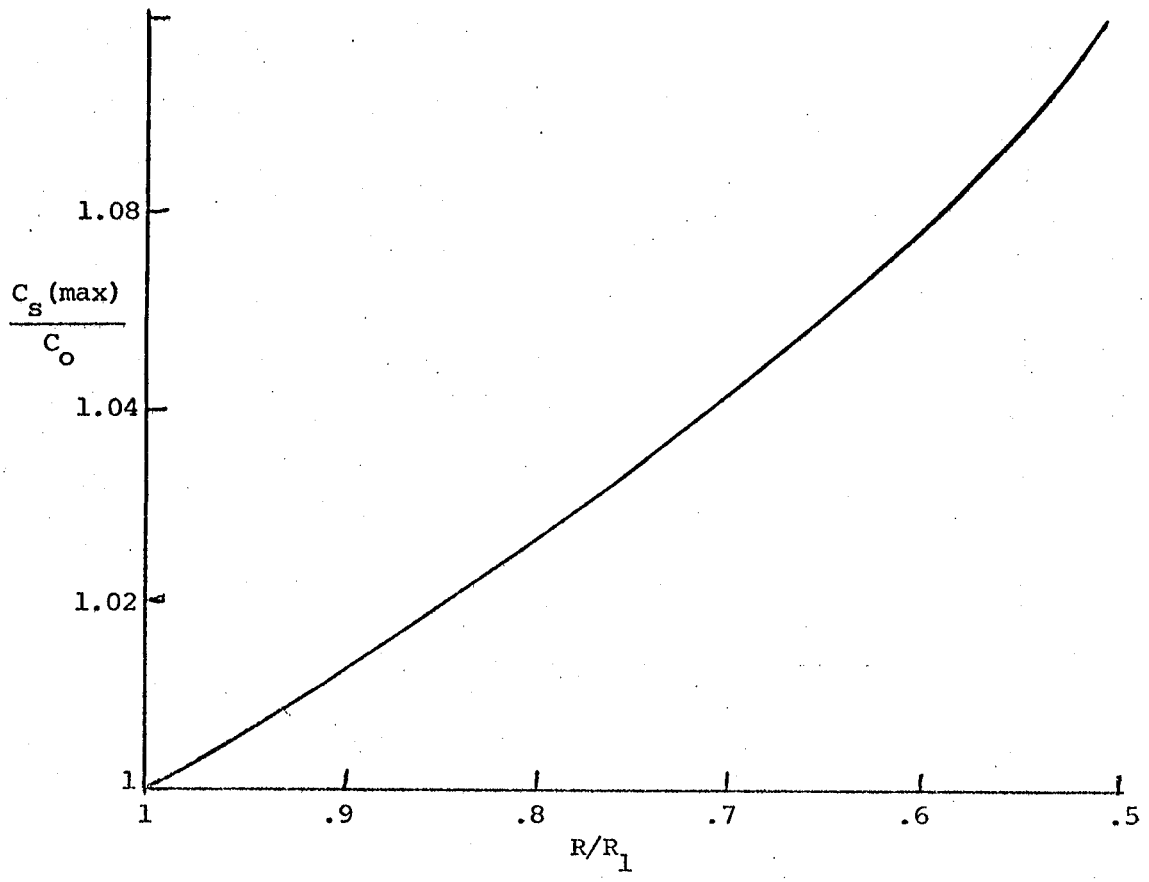

Figure 9.- Calculated maximum compositional variation as a function of growth rate change for $Pb_{.8}Sn_{.2}Te$.

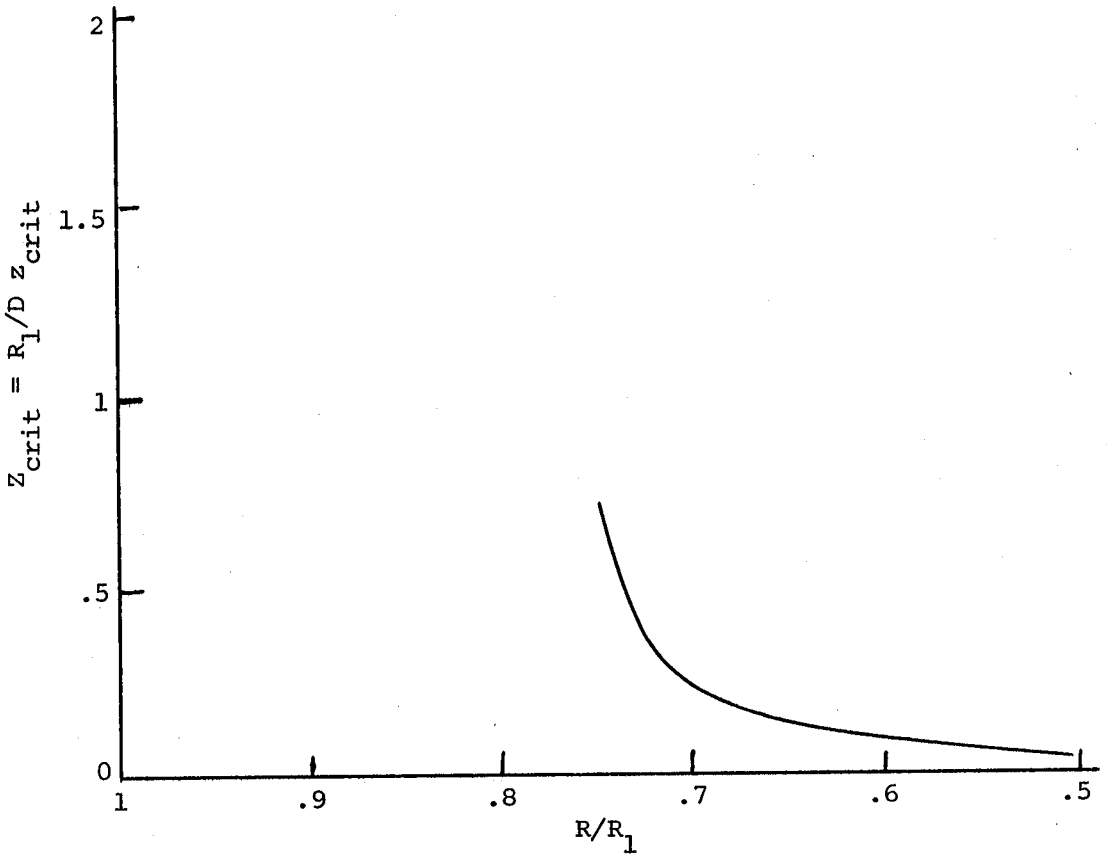

Figure 10.- Calculated dependence of the critical value of dimensionless length or ground rate change.

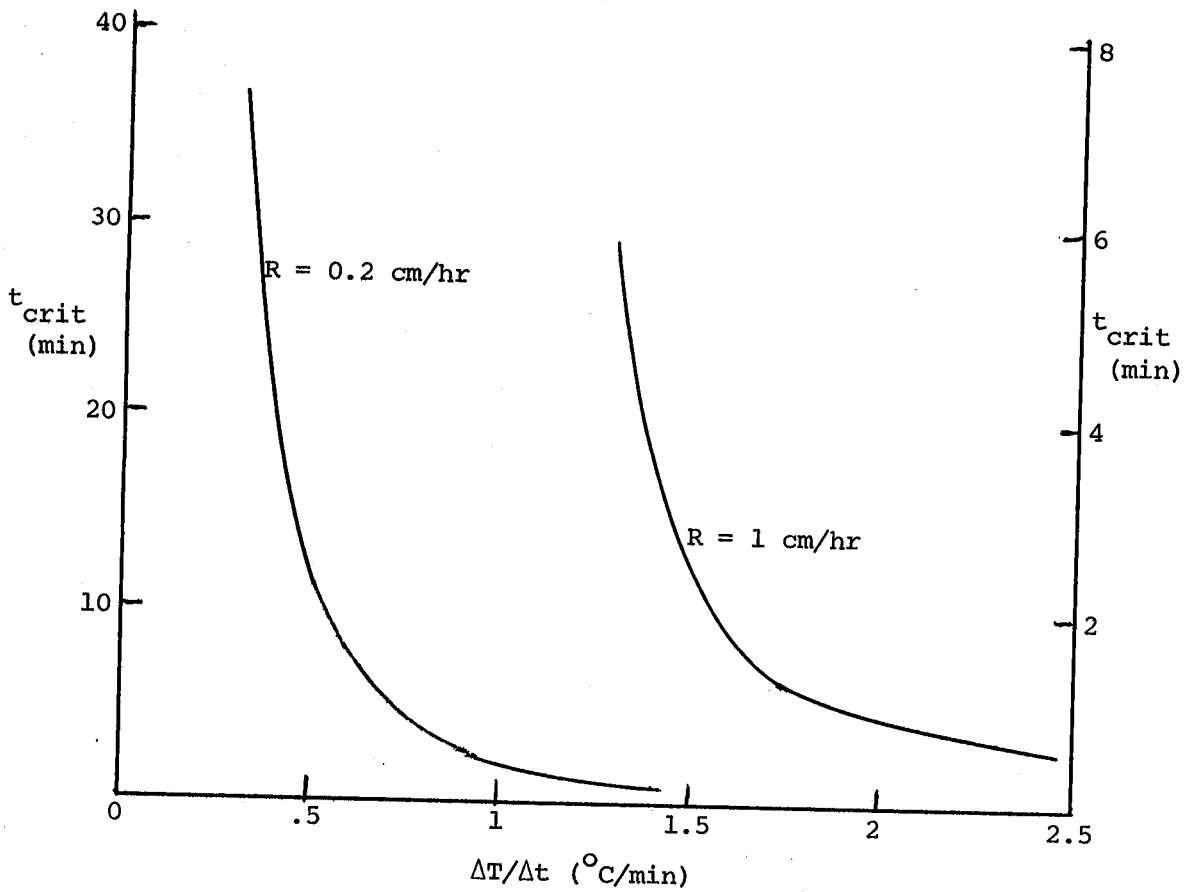

Figure 11.- Calculated relationship between temperature perturbation and time to reach critical compositional change.

1. Report No.	2. Government Accession No.	3. Recipient's Catalog No.
NASA TM-81943		

4. Title and Subtitle	5. Report Date
EXPERIMENT REQUIREMENTS AND IMPLEMENTATION PLAN (ERIP) FOR SEMICONDUCTOR MATERIALS GROWTH IN LOW-G ENVIRONMENT EXPERIMENT NO. MPS 77F087	February 1981
	6. Performing Organization Code 542-03-30-01
7. Author(s) Roger K. Crouch, Archibald L. Fripp, William J. Debnam, and and Ivan O. Clark	8. Performing Organization Report No.
	10. Work Unit No.
9. Performing Organization Name and Address NASA Langley Research Center Hampton, VA 23665	11. Contract or Grant No.
	13. Type of Report and Period Covered Technical Memorandum
12. Sponsoring Agency Name and Address National Aeronautics and Space Administration Washington, DC 20546	14. Sponsoring Agency Code

15. Supplementary Notes

16. Abstract

Crystals of the intermetallic compound $Pb_{1-x}Sn_xTe$ will be grown in furnaces on the Space Shuttle. This document describes the reasons for conducting this growth in space, the program of investigation to develop the space experiment and the requirements that are placed on the Space Shuttle furnace. Also included in this document are relevent thermophysical properties of $Pb_{1-x}Sn_xTe$ to the degree which they are known.

17. Key Words (Suggested by Author(s))	18. Distribution Statement
Crystal Growth Low Gravity Effects Heat and Mass Transfer	Unclassified - Unlimited Subject Category 76

19. Security Classif. (of this report)	20. Security Classif. (of this page)	21. No. of Pages	22. Price*
Unclassified	Unclassified	53	A04

* For sale by the National Technical Information Service, Springfield, Virginia 22161